28. Rejman J, Bragonzi A, Conese M. Role of clathrin- and caveolae-mediated endocytosis in gene transfer mediated by lipo- and polyplexes. *Mol Ther* 2005;**12**(3):468-74.
29. Tran N, Webster TJ. Understanding magnetic nanoparticle osteoblast receptor-mediated endocytosis using experiments and modeling. *Nanotechnology* 2013;**24**(18):185102.
30. Prabha S, Zhou WZ, Panyam J, Labhasetwar V. Size-dependency of nanoparticle-mediated gene transfection: studies with fractionated nanoparticles. *Int J Pharm* 2002;**244**(1–2):105-15.
31. Wang SH, Lee CW, Chiou A, Wei PK. Size-dependent endocytosis of gold nanoparticles studied by three-dimensional mapping of plasmonic scattering images. *J Nanobiotechnol* 2010;**8**:33.
32. Rejman J, Oberle V, Zuhorn IS, Hoekstra D. Size-dependent internalization of particles via the pathways of clathrin- and caveolae-mediated endocytosis. *Biochem J* 2004;**377**(Pt 1):159-69.
33. Wiseman J, Goddard C, McLelland D, Colledge W. A comparison of linear and branched polyethylenimine (PEI) with DCChol/DOPE liposomes for gene delivery to epithelial cells in vitro and in vivo. *Gene Ther* 2003;**10**(19):1654-62.
34. Thomas M, Lu JJ, Ge Q, Zhang C, Chen J, Klibanov AM. Full deacylation of polyethylenimine dramatically boosts its gene delivery efficiency and specificity to mouse lung. *Proc Natl Acad Sci U S A* 2005;**102**(16):5679-84.
35. Liu G, Wang Z, Lu J, Xia C, Gao F, Gong Q, et al. Low molecular weight alkyl-polycation wrapped magnetite nanoparticle clusters as MRI probes for stem cell labeling and in vivo imaging. *Biomaterials* 2011;**32**(2):528-37.
36. Suh JS, Lee JY, Choi YS, Yu F, Yang V, Lee SJ, et al. Efficient labeling of mesenchymal stem cells using cell permeable magnetic nanoparticles. *Biochem Biophys Res Commun* 2009;**379**(3):669-75.
37. Coupland PG, Fisher KA, Jones DR, Aylott JW. Internalisation of polymeric nanosensors in mesenchymal stem cells: analysis by flow cytometry and confocal microscopy. *J Control Release* 2008;**130**(2):115-20.
38. Varkouhi AK, Scholte M, Storm G, Haisma HJ. Endosomal escape pathways for delivery of biologicals. *J Control Release* 2011;**151**(3):220-8.
39. Boussif O, Lezoualc'h F, Zanta MA, Mergny MD, Scherman D, Demeneix B, et al. A versatile vector for gene and oligonucleotide transfer into cells in culture and in vivo: polyethylenimine. *Proc Natl Acad Sci* 1995;**92**(16):7297-301.
40. Kay MA, Glorioso JC, Naldini L. Viral vectors for gene therapy: the art of turning infectious agents into vehicles of therapeutics. *Nat Med* 2001;7(1):33-40.
41. Tu Y, Kim JS. A fusogenic segment of glycoprotein H from herpes simplex virus enhances transfection efficiency of cationic liposomes. *J Gene Med* 2008;**10**(6):646-54.
42. Lehner R, Wang X, Marsch S, Hunziker P. Intelligent nanomaterials for medicine: carrier platforms and targeting strategies in the context of clinical application. *Nanomedicine* 2013;**9**(6):742-57.
43. Tomitaka A, Jeun M-H, Bae S-T, Takemura Y. Evaluation of magnetic and thermal properties of ferrite nanoparticles for biomedical applications. *J Magn* 2011;**16**(2):164-8.
44. Guo RM, Cao N, Zhang F, Wang YR, Wen XH, Shen J, et al. Controllable labelling of stem cells with a novel superparamagnetic iron oxide-loaded cationic nanovesicle for MR imaging. *Eur Radiol* 2012;**22**(11):2328-37.
45. Calero M, Gutiérrrez L, Salas G, Luengo Y, Lázaro A, Acedo P, et al. Efficient and safe internalization of magnetic iron oxide nanoparticles: two fundamental requirements for biomedical applications. *Nanomedicine* 2013, pii: S1549-9634(13)00675-8.
46. Namgung R, Singha K, Yu MK, Jon S, Kim YS, Ahn Y, et al. Hybrid superparamagnetic iron oxide nanoparticle-branched polyethylenimine magnetoplexes for gene transfection of vascular endothelial cells. *Biomaterials* 2010;**31**(14):4204-13.
47. Majewski AP, Schallon A, Jerome V, Freitag R, Muller AH, Schmalz H. Dual-responsive magnetic core-shell nanoparticles for nonviral gene delivery and cell separation. *Biomacromolecules* 2012;**13**(3):857-66.
48. Fulwyler MJ. Electronic separation of biological cells by volume. *Science* 1965;**150**(3698):910-1.
49. Abts H, Emmerich M, Miltenyi S, Radbruch A, Tesch H. CD20 positive human B lymphocytes separated with the magnetic cell sorter (MACS) can be induced to proliferation and antibody secretion in vitro. *J Immunol Methods* 1989;**125**(1–2):19-28.
50. Ieda M, Fu JD, Delgado-Olguin P, Vedantham V, Hayashi Y, Bruneau BG, et al. Direct reprogramming of fibroblasts into functional cardiomyocytes by defined factors. *Cell* 2010;**142**(3):375-86.

TBX1 Mutation Identified by Exome Sequencing in a Japanese Family with 22q11.2 Deletion Syndrome-Like Craniofacial Features and Hypocalcemia

Tsutomu Ogata[1*9], Tetsuya Niihori[2,9], Noriko Tanaka[3,9], Masahiko Kawai[4], Takeshi Nagashima[5], Ryo Funayama[5], Keiko Nakayama[5], Shinichi Nakashima[1], Fumiko Kato[1], Maki Fukami[6], Yoko Aoki[2], Yoichi Matsubara[2,6]

1 Department of Pediatrics, Hamamatsu University School of Medicine, Hamamatsu, Japan, **2** Department of Medical Genetics, Tohoku University School of Medicine, Sendai, Japan, **3** Department of Pediatrics, Kurashiki Central Hospital, Kurashiki, Japan, **4** Department of Pediatrics, Kyoto University School of Medicine, Kyoto, Japan, **5** Division of Cell Proliferation, United Centers for Advanced Research and Translational Medicine, Tohoku University Graduate School of Medicine, Sendai, Japan, **6** National Research Institute for Child Health and Development, Tokyo, Japan

Abstract

Background: Although *TBX1* mutations have been identified in patients with 22q11.2 deletion syndrome (22q11.2DS)-like phenotypes including characteristic craniofacial features, cardiovascular anomalies, hypoparathyroidism, and thymic hypoplasia, the frequency of *TBX1* mutations remains rare in deletion-negative patients. Thus, it would be reasonable to perform a comprehensive genetic analysis in deletion-negative patients with 22q11.2DS-like phenotypes.

Methodology/Principal Findings: We studied three subjects with craniofacial features and hypocalcemia (group 1), two subjects with craniofacial features alone (group 2), and three subjects with normal phenotype within a single Japanese family. Fluorescence *in situ* hybridization analysis excluded chromosome 22q11.2 deletion, and genomewide array comparative genomic hybridization analysis revealed no copy number change specific to group 1 or groups 1+2. However, exome sequencing identified a heterozygous *TBX1* frameshift mutation (c.1253delA, p.Y418fsX459) specific to groups 1+2, as well as six missense variants and two in-frame microdeletions specific to groups 1+2 and two missense variants specific to group 1. The *TBX1* mutation resided at exon 9C and was predicted to produce a non-functional truncated protein missing the nuclear localization signal and most of the transactivation domain.

Conclusions/Significance: Clinical features in groups 1+2 are well explained by the *TBX1* mutation, while the clinical effects of the remaining variants are largely unknown. Thus, the results exemplify the usefulness of exome sequencing in the identification of disease-causing mutations in familial disorders. Furthermore, the results, in conjunction with the previous data, imply that *TBX1* isoform C is the biologically essential variant and that *TBX1* mutations are associated with a wide phenotypic spectrum, including most of 22q11.2DS phenotypes.

Citation: Ogata T, Niihori T, Tanaka N, Kawai M, Nagashima T, et al. (2014) *TBX1* Mutation Identified by Exome Sequencing in a Japanese Family with 22q11.2 Deletion Syndrome-Like Craniofacial Features and Hypocalcemia. PLoS ONE 9(3): e91598. doi:10.1371/journal.pone.0091598

Editor: Reiner Albert Veitia, Institut Jacques Monod, France

Received November 12, 2013; **Accepted** February 12, 2014; **Published** March 17, 2014

Copyright: © 2014 Ogata et al. This is an open-access article distributed under the terms of the Creative Commons Attribution License, which permits unrestricted use, distribution, and reproduction in any medium, provided the original author and source are credited.

Funding: This work was supported in part by grants from the Ministry of Health, Labor, and Welfare, from the Ministry of Education, Culture, Sports, Science and Technology, and from the National Center for Child Health and Development. The funders had no role in study design, data collection and analysis, decision to publish, or preparation of the manuscript.

Competing Interests: The authors have declared that no competing interests exist.

* E-mail: tomogata@hama-med.ac.jp

9 These authors contributed equally to this work.

Introduction

Chromosome 22q11.2 deletion syndrome (22q11.2DS) is a developmental disorder associated with characteristic craniofacial features with velopharyngeal incompetence, cardiovascular anomalies primarily affecting the outflow tracts, hypoparathyroidism and resultant hypocalcemia, and thymic hypoplasia leading to susceptibility to infection [1]. This condition is also frequently accompanied by non-specific clinical features such as developmental retardation [1]. Expressivity and penetrance of these features are highly variable and, consistent with this, chromosome 22q11.2 deletions have been identified in DiGeorge syndrome (DGS) and velocardiofacial syndrome (VCFS) with overlapping but different patterns of clinical features [1].

While multiple genes are involved in chromosome 22q11.2 deletions [2], *TBX1* (T-box 1) has been regarded as the major gene relevant to the development of clinical features in 22q11.2DS [3]. Indeed, heterozygous *TBX1* mutations have been identified in several deletion-negative patients with 22q11.2DS phenotype [2–8], and mouse studies argue for the critical role of *Tbx1* in the development of 22q11.2DS phenotypes [3]. However, the frequency of *TBX1* mutations remains rare in deletion-negative patients: Gong et al. identified only a few probable *TBX1* mutations after studying 40 patients with DGS/VCFS phenotypes

[4], and Zweier et al. found a single *TBX1* mutation after examining 10 patients with 22q11.2DS phenotype [8]. This indicates the presence of genetic heterogeneity in the development of 22q11.2DS phenotype in deletion-negative patients. Consistent with this, another DGS/VCFS locus has been assigned to chromosome 10p13-14 region [9]. Thus, it would be reasonable to perform a comprehensive genetic analysis in deletion-negative patients with 22q11.2DS phenotype.

In this regard, recent advance in molecular technologies has enabled to perform comprehensive genetic analyses, thereby contributing to the identification of underlying factors in genetic disorders. Indeed, genomewide array comparative genomic hybridization (CGH) has identified multiple disease-associated copy-number changes [10], and exome sequencing has discovered multiple disease-causing gene mutations [11]. In particular, these technologies can be powerful methods for familial disorders, because it is predicted that a single copy-number change or mutation is shared in common by affected subjects and is absent from non-affected subjects within a family.

Here, we performed array CGH analysis and exome sequencing in a family with 22q11.2DS-like clinical features. Although this study did not discover a novel disease gene, a *TBX1* mutation was successfully identified.

Materials and Methods

Ethics statement

The Institutional Review Board Committees of Hamamatsu University School of Medicine, Tohoku University School of Medicine, Kurashiki Central Hospital, and National Research Institute for Child Health and Development considered and approved the study, consent/assent procedures, and the publication of images and case details associated with this work. The individuals in this manuscript have given written informed consent (as outlined in PLOS consent form) to publish these case details. Actually, this study was performed after obtaining written informed consent from the parents of the child subjects and from the adult subjects. Furthermore, the mother and the elder brother aged 19 years old have given written informed consent to publication of the facial photographs of the two brothers; in addition, the younger brother aged 10 years has given informed assent.

Clinical Report

The pedigree of this Japanese family is shown in Fig. 1, and clinical findings of the family members are summarized in Table 1. The proband (subject III-5) was found to have hypocalcemia and hyperphosphatemia in a pre-operation laboratory test for repeated otitis media at 8 years of age, and was referred to Department of Pediatrics at Kurashiki Central Hospital. Subsequent examination revealed borderline low serum intact PTH value. Thus, he was diagnosed as having hypoparathyroidism, and received vitamin D therapy. Furthermore, physical examination showed characteristic craniofacial features with velopharyngeal incompetence suggestive of 22q11.2DS.

Similar craniofacial features were also exhibited by subjects II-2, III-1, III-6, and III-7, and hypocalcemia was also identified in subjects II-2 and III-7. Actually, subject II-2 was taking vitamin D, and subject III-7 was noticed to have hypocalcemia at birth because of the history of subject III-5, and was treated with vitamin D. The five subjects with 22q11.2DS-like craniofacial features lacked cardiovascular anomalies; while they also lacked susceptibility to infection, except for repeated otitis media in subject III-5, thymic hypoplasia was not evaluated in four of the five subjects. By contrast, the five subjects exhibited borderline to mild developmental delay. Indeed, adult subjects II-2 and III-1 had some difficulty in verbal communications, although they were able to get on their daily life, and subject II-2 was able to take care of family members. Similarly, child subjects III-5, III-6, and III-7 also showed speech delay, and subjects III-5 and III-7 received speech therapy. Furthermore, subject III-7 was diagnosed as having pervasive developmental disorder, and his verbal, performance, and full scale intelligence quotients were assessed as 63, 64, and 60, respectively, by the WISC-III method at 10 years of age. In addition, subject II-2 had sensorineural deafness, and subject III-5 had Graves' disease.

Molecularly Studied Subjects

Molecular studies were performed for eight subjects in this family, using peripheral blood samples. They were divided into three groups in terms of clinical findings: group 1, subjects II-2, III-5, and III-7 with craniofacial features and hypocalcemia; group 2, subjects III-1 and III-6 with craniofacial features alone; and group 3, subjects II-1, III-3, and IV-1 with apparently normal phenotype (Fig. 1).

FISH and Array CGH Analyses

Fluorescence *in situ* hybridization (FISH) analysis was performed with a probe for *HIRA* on the commonly deleted chromosome 22q11.2 region and that for *ARSA* at chromosome 22q13 utilized as an internal control (Abott). Array CGH was carried out using a genomewide 2x400K Agilent platform catalog array, according to the manufacturer's instructions (Agilent Technologies), and copy number variants/polymorphisms were screened with Agilent Genomic Workbench software using the Database of Genomic Variants (http://dgv.tcag.ca/dgv/app/home).

Exome and Sanger Sequencings

Exon capture was performed with the SureSelect Human All Exon kit v4 (Agilent Technologies). Exon libraries were sequenced with the Illumina Hiseq 2000 platform according to the manufacturer's instructions (Illumina), providing 108–122 average depth for each sample. Paired 101-base pair reads were aligned to the reference human genome (UCSChg19) using the Burrows-Wheeler Alignment tool [12]. Likely PCR duplicates were removed with the Picard program (http://picard.sourceforge.net/). Single-nucleotide variants and indels were identified using the Genome Analysis Tool Kit (GATK) v1.6 software [13]. SNVs and indels were annotated against the RefSeq database, 1000 Genomes Project variant data, and dbSNP135 with the ANNOVAR program [14].

To confirm mutations indicated by exome sequencing, Sanger sequencing was performed for PCR products obtained with primers flanking the detected mutations, using a 3500xL genetic analyzer (Life Technologies). Furthermore, the PCR products were subcloned with TOPO TA Cloning Kit (Life Technologies), and normal and mutant alleles were sequenced separately.

In silico protein functional analysis

Function of proteins with missense variations was assessed by Polymorphism Phenotyping-2 (PolyPhen-2, http://genetics.bwh.harvard.edu/pph2/) and Sorting Intolerant From Tolerant (SIFT, http://sift.jcvi.org/), and that of proteins with in-frame amino acid deletions was evaluated by PROVEAN predictions (http://provean.jcvi.org/index.php).

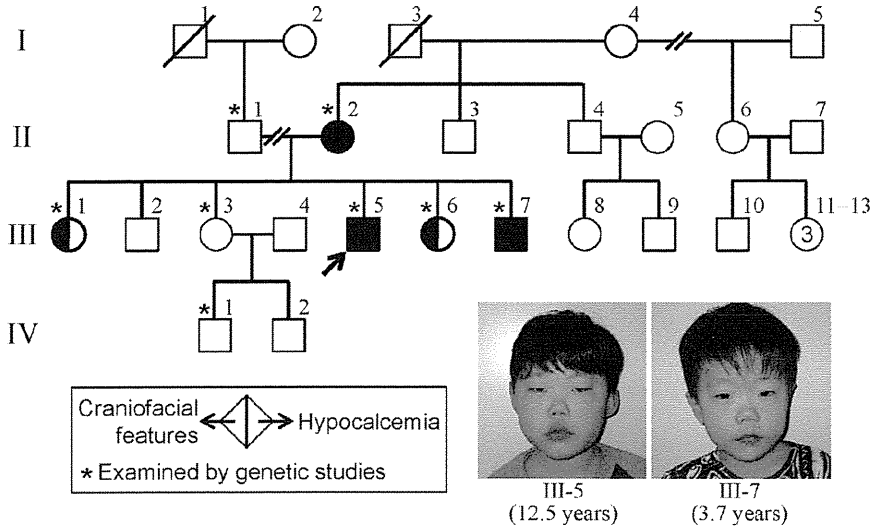

Figure 1. The pedigree of this family. Facial features of subjects III-5 and III-7 are shown.
doi:10.1371/journal.pone.0091598.g001

Results

FISH and Array CGH Analyses

FISH analysis delineated two signals for *HIRA* (Fig. 2A). Array CGH analysis revealed no copy number change specific to group 1 or groups 1+2, in the entire genome including chromosome 10p13-14 and chromosome 22q11.2 regions (Fig. 2B).

Exome and Sanger Sequencings

Exome sequencing identified nine heterozygous non-synonymous variants (six missense variants, two in-frame microdeletions, and one frameshift variant) that were specific to groups 1+2 (namely, they were present in groups 1+2 and absent from group 3 as well as from 1000 Genomes, dbSNP135, and our in-house exome data from 70 individuals) (Table S1). Notably, the frameshift variant (c.1253delA, p.Y418fsX459) was found at exon 9C of *TBX1* for DGS/VCFS (Fig. 3). Of the remaining eight variants, two variants were also detected in disease-related genes: p.G204R in *HDAC4* for brachydactyly-mental retardation syndrome [15], and p.276del in *CCND1* constituting a susceptibility factor for colorectal cancer and a modifier for von Hippel-Lindau disease [16,17]. Exome sequencing also detected two heterozygous missense variants that were specific to group 1 (Table S1).

When all variants were included, exome sequencing revealed: (1) 83 non-synonymous and 86 synonymous variants that were present in groups 1+2 and absent from group 3 (Table S2); (2) 54 non-synonymous and 48 synonymous variants that were present in group 1 and absent from groups 2+3 (Table S3); (3) 6,033 non-synonymous and 6,667 synonymous variants that were present in groups 1+2, but not specific to groups 1+2 (thus, they may be present in group 3 or absent from group 3); and (4) 7,073 non-synonymous and 7,861 synonymous variants that were present in group 1, but not specific to group 1. Furthermore, comparison of the exome sequencing data between group 1 with hypocalcemia and group 2 without hypocalcemia revealed 231 non-synonymous and 254 synonymous variants that were present in group 1 and absent from group 2 (Table S4), and 246 non-synonymous and 242 synonymous variants that were present in group 2 and absent from group 1 (Table S5). (The variant data other than those described in Supplemental Tables may be available on request after discussion with the family members and approval by our IRBs, because they contain a huge amount of individual genetic information.)

In silico protein functional analysis

The results are summarized in Table S1. The p.G204R in *HDAC4* and the p.E276del in *CCND1* were assessed as non-pathologic, while some variants were evaluated as potentially pathologic.

Discussion

Exome sequencing successfully identified a heterozygous frameshift variant on exon 9C of *TBX1*. The c.1253delA (p.Y418fsX459) appears to be a disease-causing mutation, because it is predicted that this variant escapes nonsense-mediated mRNA decay due to its position on the final exon [18] and produces a truncated protein lacking the nuclear localization signal (NLS) and most of the transactivation domain (TAD) on exon 9C (Fig. 3) [19]. In support of this, functional studies for a similar c.1223delC (p.S408fsX459) mutation on exon 9C have shown that the truncated p.S408fsX459 protein was incapable of localizing to nucleus and lost transactivation function [2,5,19]. One may argue that this c.1253delA mutation affects *TBX1* isoform C (*TBX1C*, TBX1-003) alone, while *TBX1* produces three transcript variants containing T-box [2,4] (Fig. 3). However, *TBX1C* is the major transcript with the NLS and the TAD in human and is highly homologous to mouse *Tbx1* [4] (Fig. S1).

Craniofacial features in groups 1+2 and hypocalcemia in group 1 are well explained by the *TBX1* mutation [3]. This argues for a critical role of this mutation in the phenotypic development in groups 1+2, while the clinical effects of the remaining variants identified by exome sequencing are largely unknown. In this regard, comparison between group 1 with hypocalcemia and group 2 without hypocalcemia revealed a large number of non-synonymous and synonymous variants that exclusively belonged to either group 1 (Table S4) or group 2 (Table S5), although the lists did not contain a c.2968A>G (p.R990G) SNP in *CASR* (calcium sensing receptor) that has a gain-of-function effect and appears to raise the susceptibility to hypocalcemia (Fig. S2) [20]. Thus, it is

Table 1. Clinical findings of the family members.

	TBX1 mutation (+)					*TBX1* mutation (−)			*TBX1* mutation (N.E.)		
Individual	**II-2**	**III-1**	**III-5**	**III-6**	**III-7**	**II-1**	**III-3**	**IV-1**	**II-3**	**II-4**	**III-2**
Present age (year)	51	26	19	13	10	59	22	5	50	49	25
Sex	F	F	M	F	M	M	F	M	M	M	M
Craniofacial features	+	+	+	+	+	−	−	−	−	−	−
Hypertelorism	+	+	+	+	+	−	−	−	−	−	−
Blepharophimosis	+	+	+	+	+	−	−	−	−	−	−
Low set ears	+	+	+	+	+	−	−	−	−	−	−
Auricular anomalies	+	−	−	−	−	−	−	−	−	−	−
Narrow nose	+	+	+	+	+	−	−	−	−	−	−
Cleft palate	−	−	−	−	−	−	−	−	−	−	−
Micrognathia	±	+	+	+	+	−	−	−	−	−	−
Velopharyngeal incompetence	+[d]	+	+	+	+	−	−	−	−	−	−
Hypoparathyroidism	+	−	+	−	+	−	−	−	−	−	−
Age at examination (year)	44	17	8	4	0 (1 day)	N.E.	15	0 (6 days)	N.E.	N.E.	18
Serum calcium (mg/dL)[a]	7.6[e]	9.0	6.0	9.1	5.9	...	9.0	9.8	...	...	9.6
Serum i-phosphate (mg/dL)[a]	3.9[e]	4.9	9.1	5.0	N.E.	...	4.8	6.3	...	...	4.6
Serum intact PTH (pg/dL)[a]	31[e]	N.E.	15	N.E.	19	...	N.E.	34	...	...	N.E.
Cardiovascular anomalies[b]	−	−	−	−	−	−	−	−	−	−	−
Hypoplastic thymus[c]	−	N.E.	N.E.	N.E.	N.E.	N.E.	N.E.	N.E.	N.E.	N.E.	N.E.
Susceptible to infection	−	−	−[f]	−	−	−	−	−	−	−	−
Other features	−	−	−	−	−	−	−	−	−	−	−
Developmental retardation	+	+	+[g]	+	+[g]	−	−	−	−	−	−
Sensorineural deafness	+[h]	−	−	−	−	−	−	−	−	−	−
Graves' disease	−	−	+[i]	−	−	−	−	−	−	−	−

Individuals correspond to those shown in Fig. 1.
i-phosphate: inorganic phosphate; SD: standard deviation; F: female; M: male; and N.E.: not examined.
[a]Reference values: calcium, 9.0–11.0 mg/dL in infants and 8.8–10.2 mg/dL in adults; inorganic phosphate, 4.8–7.5 mg/dL in infants and 2.5–4.5 mg/dL in adults, and intact PTH, 10–65 pg/dL in infants and 14–55 pg/dL in adults.
Conversion factor to the SI unit: 0.25 for calcium (mmol/L), 0.32 for inorganic phosphate (mmol/L), and 0.106 for intact PTH (pmol/L).
[b]Examined by echocardiography, chest roentgenography, and/or electrocardiography.
[c]Examined by computed tomography.
[d]Received velopharyngeal closure.
[e]On treatment with vitamin D.
[f]Repeated otitis media only.
[g]Received speech therapy.
[h]Required hearing aids.
[i]At the time of diagnosis (11 years of age), serum TSH was <0.01 mIU/L, free T_3 33.1 pg/mL [51.0 pmol/L], free T_4 5.11 ng/dL [65.8 nmol/L], and TSH receptor antibody 1284% [normal range <1.9%].
doi:10.1371/journal.pone.0091598.t001

likely that, together with environmental factors, the combination of hitherto unknown calcium metabolism-related functional variants would underlie different serum calcium values between groups 1 and 2.

In addition to craniofacial features with and without hypocalcemia, *TBX1* mutation positive subject II-2 had sensorineural deafness, and III-5 had Graves' disease. Since such features are occasionally manifested by patients with 22q11.2DS [21,22], the results may suggest the relevance of *TBX1* to such rather infrequent features in 22q11.2DS.

The five *TBX1* mutation positive subjects in groups 1+2 lacked cardiovascular lesion and manifested borderline to mild developmental retardation (while they had no susceptibility to infection, assessment of thymic hypoplasia remained fragmentary). By contrast, cardiovascular lesion is frequently observed and developmental retardation is rare in previously reported patients with *TBX1* mutations, although clinical features are fairly variable among mutation positive patients (Table 2). Such difference would more or less be ascribed to an examination bias that *TBX1* has been analyzed in patients with isolated cardiovascular lesion in several studies [4,6,7] or to the functional difference of the mutant proteins [2,5–8]. However, in seven patients who have been examined for DGS/VCFS-like clinical features and found to have frameshift mutations on exon 9C (p.S408fsX459, p.H425fsX613, and p.S431fsX608) affecting the NLS and the TAD, cardiovascular lesion was present in four patients and developmental delay was absent or not described, despite apparent similarity in the ascertainment of patients and the function of mutant proteins between the seven patients and the five affected subjects in this family (Table 2) [2–5].

Thus, there may be protective factor(s) for cardiovascular lesion and susceptibility factor(s) for developmental delay in groups 1+2.

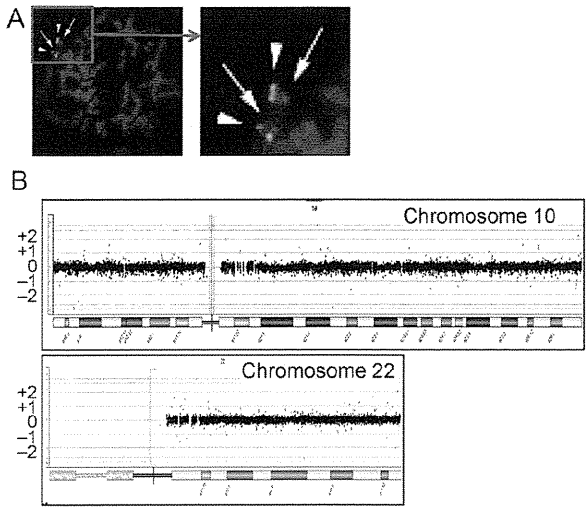

Figure 2. FISH and array CGH analyses in the proband (III-5). A. FISH analysis. Two signals are shown for both *HIRA* at 22q11.2 (red signals indicated by arrows) and *ARSA* at 22q13 (green signals indicated by arrowheads). **B.** Array CGH analysis. No copy number change is found for chromosome 10 carrying the second DiGeorge region and chromosome 22 harboring the DGS/VCFS critical region, as well as other chromosomes (not shown). Black, red, and green dots denote signals indicative of the normal, the increased (>+0.5), and the decreased (<−0.8) copy numbers, respectively. Although several red and green signals are seen, there is no portion associated with ≥3 consecutive red or green signals.
doi:10.1371/journal.pone.0091598.g002

In this regard, a simple explanation would be that protective factor(s) for cardiovascular lesion are present in groups 1+2 and may be present in group 3 or absent from group 3, whereas susceptibility factor(s) for developmental delay is present in groups 1+2 and absent from group 3. Since 6,033 non-synonymous and 6,667 synonymous variants were found to be present in groups 1+2 but not specific to groups 1+2, and 83 non-synonymous and 86 synonymous variants were revealed to be present in groups 1+2 and absent from group 3, a certain fraction of functional variants may constitute protective factor(s) for cardiovascular lesion and susceptibility factor(s) for developmental delay. In addition, while p.G204R on *HDAC4* for brachydactyly-mental retardation syndrome was assessed as non-pathologic by *in silico* analysis, it may have played a certain role in the occurrence of developmental delay in groups 1+2. Actually, such protective and susceptibility factor(s) would be more complex, with the effects of functional variants unique to each patient as well as the influences of environmental factors. Furthermore, it remains possible that the c.1253delA (p.Y418fsX459) mutation found in this study may be related to a specific phenotype characterized by the presence of craniofacial features and developmental delay and by the absence of cardiovascular lesion, because of a hitherto unrevealed mechanism(s). This matter awaits further studies.

Besides the clinical findings, several matters are also notable in the nine apparently pathologic *TBX1* mutations identified to date (Table 2). First, the mutations reside on exons 3–8 common to isoforms A–C or on exon 9C specific to isoform C, with no mutation on exons 9A and 9B specific to isoforms A and B. This would be consistent with *TBX1C* having the primary biological function. Second, while most mutations have loss-of-function effects, gain-of-function effects have been suggested for p.F148Y, p.H194Q, and p.310S by *in vitro* studies [8]. Thus, *TBX1* loss-of-function mutations and gain-of-function mutations may result in overlapping clinical features. Lastly, the c.1274_1281delACTATCTC (p.H425fsX613) missing the NLS on exon 9C was shared by a patient with DGS-like phenotype and the apparently normal mother, and the c.129_185del57 (p.43-61del19) with reduced transcriptional activity was common to a patient with non-syndromic tetralogy of Fallot and the apparently normal mother. This would imply the reduced penetrance of phenotypes caused by these mutations.

In summary, we identified a *TBX1* mutation by exome sequencing in a family with chromosome 22q11.2 deletion-like

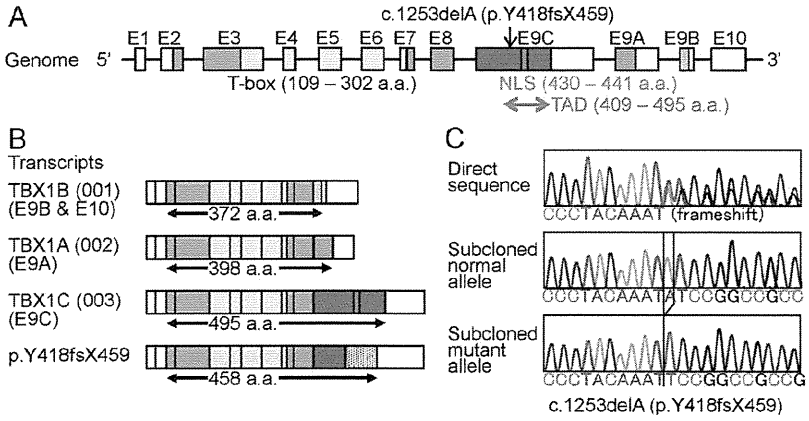

Figure 3. *TBX1* mutation identified in this family. A. Genomic structure of *TBX1* and the position of the mutation. The color and the white boxes represent the coding regions and the untranslated regions on exons 1–10 (E1–E10), respectively; the red, the purple, and the orange segments indicate the coding regions on the final exons 9C, 9A, and 9B (splice variants), respectively. The T-box is indicated by yellow boxes, the nuclear localization signal (NLA) by a blue segment, and the transactivation domain (TAD) by a green arrow. The c.1253delA (p.Y418fsX459) identified in this family resides on exon 9C. **B.** Transcripts of *TBX1*. Three variants are formed by alternative splicing of the final exons 9C, 9A, and 9B. The c.1253delA (p.Y418fsX459) mutation is predicted to yield a truncated TBX1C protein missing the NLS and most of the TAD. The stippled box of p.Y418fsX459 denotes aberrant amino acid sequence produced by the frameshift mutation. **C.** Electrochromatograms showing the frameshift mutation by Sanger sequencing. The primer sequences used are: 5′-GCGGCCAAGAGCCTTCTCT-3′ and 5′-GGGTGGTAGCCGTGGCCA-3′.
doi:10.1371/journal.pone.0091598.g003

Table 2. Summary of patients with *TBX1* mutations.

	TBX1C only					TBX1A–C				22q11.2DS
Position	**Exon 9C**	**Exon 9C**	**Exon 9C**	**Exon 9C**	**Exon 9C**	**Exon 3**	**Exon 4**	**Exon 5**	**Exon 8**	
cDNA change[a]	c.1223	c.1253	c.1274_1281	c.1293_1315	c.1399_1428	c.129_185	c.443T>A	c.582C>G	c.928G>A	Deletion
	delC	delA	del8	del23[h]	dup30[k]	del57[k]				
Amino acid	p.S408	p.Y418	p.H425	p.S431	p.467_476	p.43_61	p.F148Y	p.H194Q	p.G310S	
change	fsX459	fsX459	fsX613	fsX608	dup10A	del19				
NLS (exon 9C)	–	–	–	+[i]	+[l]	+	+	+	+	
TAD (exon 9C)	–	Involved	Involved	Involved	Involved	+	+	+	+	
Function	LOF	N.E.	N.E.	LOF	LOF	Reduced	GOF[m]	GOF[m]	GOF[m]	
Patient number	3	5	1	3[j]	2	1	1	2	1	558
Occurrence	Familial	Familial	Sporadic[g]	Familial	Sporadic	Sporadic[g]	Sporadic	Familial	Sporadic	
Facial features[b]	3/3	5/5	+	3/3	0/2	–	+	2/2	+	100%
Nasal voice[c]	2/3	5/5	N.D.	3/3	0/2	–	+	0/2	+	32%
Cardiovascular anomalies	1/3	0/5	+	2/3	2/2	+	+	0/2	+	57%
Hypopara-thyroidism[d]	1/3	3/5	+	N.D.	0/2	–	–	0/2	+	60%
Hypoplastic thymus	1/2[e]	0/1[f]	+	N.D.	0/2	–	–	N.E.	+	?
Susceptible to infection	N.D.	0/5	N.D.	N.D.	0/2	–	N.D.	N.D.	N.D.	?
Developmental retardation	0/3	5/5	N.D	0/3	0/2	–	–	1/2	–	38%
Reference	2	This study	3, 4	5	4, 6	7	2	8	2	1

In addition to the mutations listed in this table, several missense variants and in-frame indels with unknown functions have been found in patients with isolated cardiovascular anomalies and in those with DGS/VCFS-like phenotype [4].
NLS: nuclear localization signal; TAD: transactivation domain; LOF: loss-of-function; N.D.: not described; N.E.: not examined; GOF: gain-of-function; Del: deletion; and Dup: duplication.
[a]According to NM_080647.
[b]Suggestive of 22q11.2 deletion syndrome.
[c]Velopharygeal insufficiency.
[d]Hypocalcemia is included.
[e]Two of the three subjects have been examined for hypoplastic thymus.
[f]One of the five subjects has been examined for hypoplastic thymus.
[g]These two mutations have been inherited from apparently normal mothers.
[h]The c.1293-1315del23 has been described as c.1320-1342del23 in the original report [5].
[i]Although the natural NLS has been disrupted, a new NLS-compatible motif (RGRRRRCR) has been created on the added amino acid sequence.
[j]Another deceased individual in this family also has similar clinical features.
[k]These two mutations have been identified in *TBX1* analyses for patients with cardiovascular anomalies only.
[l]The mutant protein is aggregated in the cytoplasm and the nucleus.
[m]Gain-of-function effects have been found by *in vitro* studies [8].
doi:10.1371/journal.pone.0091598.t002

phenotype. Application of such powerful methods will serve to identify a causative gene in genetically heterogeneous disorders.

Supporting Information

Figure S1 Comparison of amino acid sequence of human *TBX1C* and mouse *Tbx1*. The T-box is highlighted in yellow, and the nuclear localization signal in light blue. The region for transactivation domain is surrounded by squares. The Y highlighted in red denotes the amino acid residue where the frameshift mutation in this family has taken place.
(TIF)

Figure S2 Analysis of c.2968A>G SNP (p.R990G, rs1042636) with a gain-of-function effect in exon 7 of *CASR*. The SNP pattern is not co-segregated with the presence or absence of hypocalcemia.
(TIF)

Table S1 Summary of heterozygous non-synonymous variants.
(PDF)

Table S2 A list of variants that are present in groups 1+2 and absent from group 3.
(PDF)

Table S3 A list of variants that are present in group 1 and absent from groups 2+3.
(PDF)

Table S4 A list of variants that are present in group 1 and absent from group 2.
(PDF)

Table S5 A list of variants that are present in group 2 and absent from group 1.
(PDF)

References

1. Ryan AK, Goodship JA, Wilson DI, Philip N, Levy A, et al. (1997) Spectrum of clinical features associated with interstitial chromosome 22q11 deletions: a European collaborative study. J Med Genet 34: 798–804.
2. Yagi H, Furutani Y, Hamada H, Sasaki T, Asakawa S, et al. (2003) Role of TBX1 in human del22q11.2 syndrome. Lancet 362: 1366–1373.
3. Baldini A (2005) Dissecting contiguous gene defects: TBX1. Curr Opin Genet Dev 15: 279–84.
4. Gong W, Gottlieb S, Collins J, Blescia A, Dietz H, et al. (2001) Mutation analysis of TBX1 in non-deleted patients with features of DGS/VCFS or isolated cardiovascular defects. J Med Genet 38: E45.
5. Paylor R, Glaser B, Mupo A, Ataliotis P, Spencer C, et al. (2006) Tbx1 haploinsufficiency is linked to behavioral disorders in mice and humans: implications for 22q11 deletion syndrome. Proc Natl Acad Sci U S A 103: 7729–7734.
6. Rauch R, Hofbeck M, Zweier C, Koch A, Zink S, et al. (2010) Comprehensive genotype-phenotype analysis in 230 patients with tetralogy of Fallot. J Med Genet 47: 321–331.
7. Griffin HR, Töpf A, Glen E, Zweier C, Stuart AG, et al. (2010) Systematic survey of variants in TBX1 in non-syndromic tetralogy of Fallot identifies a novel 57 base pair deletion that reduces transcriptional activity but finds no evidence for association with common variants. Heart 96: 1651–1655.
8. Zweier C, Sticht H, Aydin-Yaylagül I, Campbell CE, Rauch A (2007) Human TBX1 missense mutations cause gain of function resulting in the same phenotype as 22q11.2 deletions. Am J Hum Genet 80: 510–517.
9. Daw SCM, Taylor C, Kraman M, Call K, Mao J, et al. (1996) A common region of 10p deleted in DiGeorge and velocardiofacial syndromes. Nat Genet 13: 458–461.
10. McDonnell SK, Riska SM, Klee EW, Thorland EC, Kay NE, et al. (2013) Experimental designs for array comparative genomic hybridization technology. Cytogenet Genome Res 139: 250–257.
11. Wang Z, Liu X, Yang B-Z, Gelernter J (2013) The role and challenges of exome sequencing in studies of human diseases Front Genet doi: 10.3389/fgene.2013.00160.
12. Li H, Durbin R (2009) Fast and accurate short read alignment with Burrows-Wheeler transform. Bioinformatics 25: 1754–1760.
13. McKenna A, Hanna M, Banks E, Sivachenko A, Cibulskis K, et al. (2010) The Genome Analysis Toolkit: a MapReduce framework for analyzing next-generation DNA sequencing data. Genome Res 20: 1297–1303.
14. Wang K, Li M, Hakonarson H (2010) ANNOVAR: functional annotation of genetic variants from high-throughput sequencing data. Nucleic Acids Res 38: e164.
15. Williams SR, Aldred MA, Der Kaloustian VM, Halal F, Gowans G, et al (2010). Haploinsufficiency of HDAC4 causes brachydactyly mental retardation syndrome, with brachydactyly type E, developmental delays, and behavioral problems. Am J Hum Genet 87: 219–228.
16. Kong S, Amos CI, Luthra R, Lynch PM, Levin B, et al. (2000) Effects of cyclin D1 polymorphism on age of onset of hereditary nonpolyposis colorectal cancer. Cancer Res 60: 249–252.
17. Zatyka M, da Silva NF, Clifford SC, Morris MR, Wiesener MS, et al (2002). Identification of cyclin D1 and other novel targets for the von Hippel-Lindau tumor suppressor gene by expression array analysis and investigation of cyclin D1 genotype as a modifier in von Hippel-Lindau disease. Cancer Res 62: 3803–3811.
18. Holbrook JA, Neu-Yilik G, Hentze MW, Kulozik AE (2004) Nonsense-mediated decay approaches the clinic. Nat Genet 36: 801–808.
19. Stoller JZ, Epstein JA (2005) Identification of a novel nuclear localization signal in Tbx1 that is deleted in DiGeorge syndrome patients harboring the 1223delC mutation. Hum Mol Genet 14: 885–892.
20. Vezzoli G, Terranegra A, Arcidiacono T, Biasion R, Coviello D, et al. (2007) R990G polymorphism of calcium-sensing receptor does produce a gain-of-function and predispose to primary hypercalciuria. Kidney Int 71: 1155–1162.
21. Ohtani I, Schuknecht HF (1984) Temporal bone pathology in DiGeorge's syndrome. Ann Otol Rhinol Laryngol 93(3 Pt 1): 220–224.
22. Kawame H, Adachi M, Tachibana K, Kurosawa K, Ito F, et al. (2001) Graves' disease in patients with 22q11.2 deletion. J Pediatr 139: 892–895.

Author Contributions

Conceived and designed the experiments: TO YM. Performed the experiments: T. Niihori SN FK MF YA. Analyzed the data: T. Nagashima RF KN. Contributed reagents/materials/analysis tools: KN. Wrote the manuscript: TO. Collected the clinical findings: NT MK.

JIMD Reports
DOI 10.1007/8904_2014_320

RESEARCH REPORT

Seven Novel Mutations in Bulgarian Patients with Acute Hepatic Porphyrias (AHP)

Sonya Dragneva • Monika Szyszka-Niagolov • Aneta Ivanova • Lyudmila Mateva • Rumiko Izumi • Yoko Aoki • Yoichi Matsubara

Received: 23 February 2014 / Revised: 07 May 2014 / Accepted: 09 May 2014 / Published online: 6 July 2014
© SSIEM and Springer-Verlag Berlin Heidelberg 2014

Abstract Acute intermittent porphyria (AIP), variegate porphyria (VP), and hereditary coproporphyria (HCP) are caused by mutations in the hydroxymethylbilane synthase (HMBS), protoporphyrinogen oxidase (PPOX), and coproporphyrinogen oxidase (CPOX) genes, respectively. This study aimed to identify mutations in seven Bulgarian families with AIP, six with VP, and one with HCP. A total of 33 subjects, both symptomatic ($n = 21$) and asymptomatic ($n = 12$), were included in this study. The identification of mutations was performed by direct sequencing of all the coding exons of the corresponding enzymes in the probands. The available relatives were screened for the possible mutations. A total of six different mutations in HMBS were detected in all seven families with AIP, three of which were previously described: c.76C>T [p.R26C] in exon 3, c.287C>T [p.S96F] in exon 7, and c.445C>T [p.R149X] in exon 9. The following three novel HMBS mutations were found: c.345-2A>C in intron 7–8, c.279-280insAT in exon 7, and c.887delC in exon 15. A total of three different novel mutations were identified in the PPOX gene in the VP families: c.441-442delCA in exon 5, c.917T>C [p.L306P] in exon 9, and c.1252T>C [p.C418R] in exon 12. A novel nonsense mutation, c.364G>T [p.E122X], in exon 1 of the CPOX gene was identified in the HCP family. This study, which identified mutations in Bulgarian families with AHP for the first time, established seven novel mutation sites. Seven latent carriers were also diagnosed and, therefore, were able to receive crucial counseling to prevent attacks.

Abbreviations

AHP	Acute hepatic porphyrias
AIP	Acute intermittent porphyria
ALA	δ-Aminolevulinic acid
CPOX	Coproporphyrinogen oxidase
HCP	Hereditary coproporphyria
HMBS	Hydroxymethylbilane synthase
PBG	Porphobilinogen
PPOX	Protoporphyrinogen oxidase
VP	Variegate porphyria

Introduction

Acute intermittent porphyria (AIP) (OMIM 176000), variegate porphyria (VP) (OMIM 176200), and hereditary coproporphyria (HCP) (OMIM 121300) are autosomal dominant, low-penetrant inborn errors of the heme biosynthesis pathway that result in the decreased activity of hydroxymethylbilane synthase (HMBS) (EC 4.3.1.8), protoporphyrinogen oxidase (PPOX) (EC 1.3.3.4), and coproporphyrinogen oxidase (CPOX) (EC 1.3.3.3), respectively.

AIP, VP, and HCP present with clinically identical recurrent neurovisceral attacks. Additionally, erosive bullous cutaneous lesions and hyperpigmentation on sun-exposed areas are more common in VP than in HCP (Sassa 2006). The acute attacks include three major classes of symptoms: gastrointestinal, neurological, and psychiatric. These symptoms are represented by severe abdominal pains, motor neuropathy, depression, and psychosis. The most common factor trigger-

Communicated by: Eva Morava, MD PhD

Competing interests: None declared

S. Dragneva (✉) · M. Szyszka-Niagolov · A. Ivanova · L. Mateva
Clinic of Gastroenterology and Hepatology, University Hospital "Saint Ivan Rislki", Sofia, Bulgaria
e-mail: sonya.dragneva@gmail.com

R. Izumi · Y. Aoki · Y. Matsubara
Department of Medical Genetics, School of Medicine, Tohoku University, Sendai, Japan

ing these attacks is the use of numerous porphyrinogenic drugs. Infections, alcohol, a low-calorie diet, and natural sex hormones fluctuations in women, related to menstrual cycle and pregnancy can also provoke attacks (Kappas et al. 1995).

The diagnosis of acute porphyric attack is based on both clinical manifestations and typical biochemical abnormalities. The main laboratory finding is the dramatic increase of the porphyrin precursors porphobilinogen (PBG) and δ-aminolevulinic acid (ALA) in urine. The exact distinction between the three different diseases requires measuring the urinary and fecal porphyrin excretion patterns, which are characteristic for each enzymatic defect. A fluorescence scan of native plasma is also an important diagnostic criterion, presenting (or not) a characteristic peak for each entity (Sassa 2006; Hift et al. 2004). Decreased levels of HMBS activity in AIP, PPOX activity in PV, and CPOX activity in HCP clarify the diagnosis in the proband and establish the enzymatic defect in the latent carriers (Meyer et al. 1972; Deybach et al. 1981). Unfortunately, when measuring enzymatic activities, results similar to the reference values may bring in uncertainty in the precise diagnosis of the latent carriers (Mustajoki 1981). Thus, the optimal strategy for the detection of these individuals includes the implementation of molecular genetic methods (Whatley et al. 2009).

At least 600 different mutations in the HMBS, PPOX, and CPOX genes have been identified so far (www.hgmd.cf.ac.uk). Most of these mutations are specific to one or a few families, although a founder effect has been clearly demonstrated for both AIP and VP (Thunnel et al. 2006; Meissner et al. 1996). Most AIP, VP, and HCP carriers are heterozygotes. Mutations are heterogeneous and are comprised of single nucleotide substitutions, small insertions and deletions. Recently, large insertions/deletions have been described in the HMBS, PPOX, and CPOX genes (Whatley et al. 2009; Barbaro et al. 2013). In Bulgaria, during a 50-year period as the sole porphyria service at University Hospital "Saint Ivan Rislki" Sofia, 35 families with AIP, 20 with VP, and 2 with HCP have been diagnosed, treated, and followed up. However, the molecular analysis of the patients with AIP, VP, and HCP has not yet been performed. The aim of this study was to identify mutations in the HMBS, PPOX, and CPOX genes in Bulgarian families with acute hepatic porphyrias.

Materials and Methods

Patients

Seven independent index cases with AIP were included. The diagnosis was based on clinical symptoms and increased urinary PBG and ALA values. Decreased levels of HMBS activity in erythrocytes and the absence of a plasma fluorescence peak at 624–627 nm confirmed the diagnosis of AIP. Six independent index cases with VP were also studied. The diagnosis of these patients included the evaluation of the clinical symptoms, a typical plasma fluorescence peak at 624–627 nm, elevated urinary PBG and ALA levels during acute attacks and increased stool porphyrins, with a predominance of protoporphyrin over coproporphyrin in the cases with cutaneous symptoms. One patient with HCP was included. The diagnosis was based on the symptoms that occurred during acute attack, increased urinary PBG and ALA levels, markedly increased total porphyrins in the urine, and a plasma fluorescence peak at 618 nm. Molecular analysis of the HMBS, PPOX, and CPOX genes confirmed the precise diagnosis. These 14 probands were diagnosed, treated, and followed up in the Porphyria Unit of "Saint Ivan Rilski" University Hospital Sofia. The precise places of birth and the pedigree trees of the patients were determined, with no apparent signs of consanguinity. Once the diagnosis of AIP was confirmed, the HMBS activity was evaluated in the available asymptomatic family members. A total of 33 individuals, including the probands and asymptomatic relatives, from 15 families with AIP, VP, and HCP gave their written consent to participate in this study, which was approved by the Ethics Committee.

Methods

Biochemical Measurements

PBG and ALA levels in the urine were measured according to the method described by Mauzarell and Granick (1956). Urinary and fecal porphyrins were assessed according to the method of Rimington (1971). Total fecal total porphyrin levels were measured according to the method of Lockwood et al. (1985). Total porphyrin levels in urine were evaluated according to our modification and optimization of the method described by Deacon and Elder (2001). HMBS activity in the erythrocytes was determined according to the method described by Adjarov et al. (1994). Plasma fluorescence scanning was performed on a Perkin–Elmer fluorescence spectrophotometer MPF 43, with an excitation wavelength of 398 nm and an emission spectrum from 580 to 700 nm.

Identification of Mutations

Genomic DNA was isolated from peripheral whole blood samples using the innuPREP Blood DNA Midi kit (Analytik Jena Life Science, Germany) according to the manufacturer's protocol. PCR amplification of exons 1 to

Table 1 Clinical and biochemical data and mutations detected in the HMBS gene in families with acute intermittent porphyria

Fam	Pts	Sex	Age/age at first symptoms	Nucleotide change	Amino acid change	Symptoms	HMBS	No. of acute attacks	Urine		TF	TT
									PBG	ALA		
I	P1	F	40/19	c.76C>T	p.R26C	+	18.7	1	715	95	MC	Glu
	Fa	M	65/44	c.76C>T	p.R26C	+	20.1	–	129	122	Inf + M	–
II	P2	F	47/20	c.279-280insAT[a]	Frameshift	+	14.1	2	153	42.7	–	C + Glu
	Sc1	F	45/26	c.279-280insAT[a]	Frameshift	+	10	2	189	–	P	Glu
	Sc2	F	37/30	c.279-280insAT[a]	Frameshift	+	14.3	1	304	–	Inf + M	Glu
	Mo	F	69	c.279-280insAT[a]	Frameshift	–	14	–	–	–	–	–
III	P3	F	44/24	c.887delC[a]	Frameshift	+	20.6	1	320	19.4	MC	Hem
	So	M	20	Neg		–	34.3	–	–	–	–	–
IV	P4	F	27/22	c.445C>T	p.R149X	+	ND	2	955	100	MC	Glu
	Mo	F	50	c.445C>T	p.R149X	+	ND	–	350	78	MC	–
	Si	F	28	Neg	–	–	ND	–	–	–	–	–
V	P5	F	59/39	c.345-2A>C[a]	Splice acceptor site	+	18.7	1	341	214	Inf + M	C + Glu
VI	P6	F	43/25	c.287C>T	p.S96F	+	25.1	1	421	45	MC	Glu
	D	F	21	c.287C>T	p.S96F	–	ND	–	–	–	–	–
VII	P7	F	42/28	c.287C>T	p.S96F	+	ND	1	384	130	MC	Glu
	D	F	15	c.287C>T	p.S96F	–	ND	–	18.2	–	–	–

Fam family, *Pts* patients, *P* proband number, *Fa* father, *Sc* second cousin, *Mo* mother, *So* son, *Si* sister, *D* daughter, *F* female, *M* male, *HMBS* hydroxymethylbilane synthase activity in the erythrocytes, normal range: 25–45 pkat/gHb, *PBG* porphobilinogen, normal value: <15 μmol/24 h, *ALA* δ-aminolevulinic acid, normal range: 11.4–57.2 μmol/24 h, *TF* triggering factor, *Inf* infection, *M* medication, *MC* menstrual cycle, *P* pregnancy, *TT* treatment, Glu, 10% glucose i.v. infusion, *C* cimetidine, *Hem* Hem-arginate (Normosang), *ND* not determined

[a] Novel mutations identified

15 for HMBS, exons 1 to 13 for PPOX, and exons 1 to 7 for CPOX, with corresponding flanking intron–exon boundaries, was performed; the primers and PCR conditions are available upon request. The PCR products were automatically sequenced using the BigDye Terminator v3.1 Cycle Sequencing Kit and a 3500xL Genetic Analyzer (Applied Biosystems, Foster City, USA).

To prove the rarity of the identified novel missense mutations, the corresponding exons of the HMBS and PPOX genes were screened in 96 control DNA samples. In silico prediction of the pathogenicity of these mutations was determined by the HumVar score using the PolyPhen-2 tool (http://genetics.bwh.harvard.edu/pph2/).

Results and Discussion

Detailed clinical, biochemical, and genetic data are presented in Table 1 for the AIP families and in Table 2 for the VP and HCP families. In three of our female AIP patients, the attacks were related to the patient's menstrual cycle. Infections and/or medications played a triggering role in three AIP and four VP cases, as well as in the HCP patient. Nine subjects with AIP manifested with one or two acute attacks. Some patients (family I-F, family II-P2 and II-Sc1, family IV-P4 and family V-P5) suffered chronic symptoms, including fatigue, lower back pain, paresthesia in the lower limbs, and depression. The proband P2 had suffered from two unrecognized acute attacks and had residual paresis at the time of presentation in our clinic. She also had chronic neurological symptoms when Cimetidine treatment was applied. During the 6 months course of Cimetidine administration, a reduction in porphyrin precursors levels and clinical improvement was achieved. Family V-P5 suffered from one acute attack following infection and antibiotic treatment after surgery. She also had chronic neurological symptoms. Cimetidine was administered after the acute onset, but over the first weeks the pains worsened and no biochemical improvement was noticed. Both acute and cutaneous symptoms were present in four symptomatic VP patients, and only acute symptoms were present in one patient and only cutaneous symptoms in four patients. All VP patients manifested with a single acute attack, and only family III-So exhibited chronic symptoms similar to those observed in AIP. The majority of our VP patients presented with severe photodermatosis alone or accompanying acute

Table 2 Clinical, biochemical and genetic characteristics of families with variegate porphyria and hereditary coproporphyria

Fam	Pts	Sex	Age/age at first symptom	Gene	Nucleotide change	Amino acid change	Symptoms		Plasma scan	Urine					Feces					
							Acute	Skin		PBG	ALA	TPu	Uro	Cop	TPf	Uro	Cop	Proto	TF	TT
I-VP	P1	F	28/21	PPOX	c.441-442delCA	Frame-shift	+	–	626	37	40	4,675	2,340	2,335	–	–	–	–	Inf + M	Glu
	D	F	11	PPOX	c.441-442delCA	Frame-shift	–	–	ND	–	–		–	–	–	–	–	–	–	–
II-VP	P2	F	30/24	PPOX	c.917T>C	p.L306P	+	+	626	383		7,076	–	–	2,422[a]	–	–	–	Inf + M	Glu
	So	M	3	PPOX	c.917T>C	p.L306P	–	–	Neg	2	13	0	–	–	0.6	–	–	–	–	–
III-VP	P3	M	69/39	PPOX	c.917T>C	p.L306P	–	+	626	3	19	1,326	143	1,183	671	84	241	346		Ph
	So	M	43/30	PPOX	c.917T>C	p.L306P	+	+	627	75	223	930	–	–	1,753	–	–	–	–	Glu
	G	M	10	PPOX	Neg	–	–	–	Neg	3	15	120	–	–	138	–	–	–	–	–
IV-VP	P4	F	80/45	PPOX	c.917T>C	p.L306P	–	+	626	2.2	16.8	1,340	79	1,261	3,182	890	662	1,630	–	Ph
	D	F	58	PPOX	c.917T>C	p.L306P	–	+	626	3.7	30	199[a]	–	–	1,202[a]	–	–	–	–	–
	So	M	48	PPOX	c.917T>C	p.L306P	–	–	Neg	5	32	0	–	–	142	–	–	–	–	–
V-VP	P5	F	31/25	PPOX	c.1252T>C	p.C418R	+	+	626	505	309	14,326	–	–	–	–	–	–	Inf + M	
	Si	F	38/25	PPOX	c.1252T>C	p.C418R	+	+	626	11[a]	33[a]	217[a]	–	–	–	–	–	–	Inf	
	So	M	19	PPOX	Neg	–	–	–	Neg	7	29	68	–	–	–	–	–	–	–	
	Ni	F	16	PPOX	c.1252T>C	p.C418R	–	–	ND	–	–		–	–	–	–	–	–	–	
	Nf	M	17	PPOX	Neg	–	–	–	ND	–	–		–	–	–	–	–	–	–	
VI-VP	P6	M	63/35	PPOX	c.1252T>C	p.C418R	–	+	626	8	66	626	74	552	268	3	88	177	–	
I-HCP	P	F	22/22	CPOX	c.364G>T	p.E122X	+	–	618	53	63	5,100	1,425	4,100	4,960	–	–	–	Inf + M	Glu

Fam, family, *Pts* patients, *P* proband number, *Si* sister, *D* daughter, *Ni* niece, *Nf* nephew, *G* grandson, *F* female, *M* male, *PBG* porphobilinogen, normal value: <15 μmol/24 h, *ALA* δ-aminolevulinic acid, normal range: 11.4–57.2 μmol/24 h, *TPu* total porphyrins in urine, normal values <200 nmol/24 h, *Plasma scan* plasma fluorescence emission peak in nm, *TPf* total porphyrins in feces, normal values <150 nmol/g dry weight, *Uro* uroporphyrin, normal values: <36 nmol/24 h in urine, <1 nmol/g dry weight in feces, *Cop* coproporphyrins, normal values: <122 nmol/24 h in urine, <26 nmol/g dry weight in feces, *Proto*, protoporphyrins, normal value: <80 nmol/g dry weight in feces, *TF* triggering factor, *Inf* infection, *M* medication, *TT* treatment, *Glu* 10% glucose i.v. infusion, *Ph* photoprotection, *ND* not determined, *Neg* no emission peak on plasma scan

[a] Mark, values measured after resolution of the acute attack

onset, with a frequency similar to that reported in South Africa and Western Europe (Whatley et al. 1999). The patient with HCP manifested with acute symptoms only. During onset, all of the patients had markedly increased levels of PBG and ALA. In all of the investigated AIP probands, except for one (family VI-P6), the HMBS activity in the erythrocytes was decreased. In P6, the HMBS activity was measured during acute onset, when transitory normal levels could be expected. Heme-arginate is not available in Bulgaria; therefore, all patients with acute onset, except for one, were treated with i.v. glucose infusions (from 200 to 500 g/day according to the severity of the attack) or Cimetidine until the clinical and biochemical parameters improved.

A total of six different mutations in HMBS were detected in all seven families with AIP, three of which were previously described as single nucleotide substitutions: c.76C > T [p.R26C] in exon 3, c.287C > T [p.S96F] in exon 7, and c.445C > T [p.R149X] in exon 9; the other three mutations were newly detected. The novel ones included a single nucleotide change, a small insertion and a single nucleotide deletion: c.345-2A > C in intron 7–8, c.279-280insAT in exon 7, and c.887delC in exon 15. Overall, there were two missense, one nonsense, one splice-site, and two frameshift mutations. The alterations identified in the Bulgarian patients were heterogeneous, as previously reported in many other populations (Whatley et al. 2009; Puy et al. 1997).

Three of the substitutions identified in the Bulgarian AIP patients have been reported in various ethnic populations. The mutations identified in families I-P1 (p.R26C) and IV-P4 (p.R149X) were initially identified in Finish patients (Kauppinen et al. 1995). p.R26C has been subsequently reported in Slavic (Hrdinka et al. 2006), Spanish (To-Figueras et al. 2006), French (Puy et al. 1997), Chinese (Yang et al. 2008), and Venezuelan populations (Paradisi and Arias 2010). The p.R149X mutation was found to be one of the relatively prevalent mutations (approximately 5%) in a large cohort of 109 mutation-positive AIP families (Puy et al. 1997). It has been shown that the R26 and R149 residues are located in the substrate-binding site and are crucial for enzymatic activity (Llewellyn et al. 1998; Gill et al. 2009). AIP family IV is of particular interest due to its gypsy origin. The gypsy people represent the largest minority in Bulgaria, and the search for the p.R149X substitution in this population deserves further attention.

In families VI-P6 and VII-P7, an identical p.S96F missense mutation was found in the HMBS gene; this mutation was first described by Kaupinnen et al. (2002). There was no significant difference in the clinical phenotype of the two probands; both patients presented with a single acute attack that was triggered by hormonal changes during their twenties. At present, both patients are symptom-free.

Novel substitutions in the HMBS gene that resulted in frameshift and splice-site alterations were identified in families II, III, and V. A small insertion (c.279-280insAT in exon 7) was identified in the II-P2 proband, resulting in a frameshift mutation that led to the formation of premature stop codon after the incorporation of 24 different amino acid residues, compared to the reference transcript. A small out-of-frame deletion (c.887delC) was identified in the III-P3 family, and this mutation led to a premature stop codon after 3 amino acids, compared to the reference sequence. The nucleotide change revealed in family V-P5 (c.345-2A>C in intron 7) affected the invariant AG acceptor splice site and possibly interfered with mRNA processing. At the same position, a different nucleotide change (c.345-2 A>G) has been reported in Swedish patients, listed in a table (Floderus et al. 2002). These three alterations have not been reported in reference databases (such as dbSNP, HGMD, 1KG, and ESP). To exclude the possibility of the novel mutations being SNPs, 96 control DNA samples were screened, and no samples revealed the presence of the novel mutations of the HMBS gene (c.345-2A>C in intron 7, c.279-280insAT in exon 7, and c.887delC in exon 15). The above finding suggests that these mutations are pathogenic. RNA analysis is needed to prove the pathogenicity of the c.345-2A > C change.

After detecting specific mutations in the families, the available family members ($n = 4$ symptomatic and $n = 5$ asymptomatic) were screened for the presence of the identified mutations (Table 1). All symptomatic relatives harbored the corresponding family-specific nucleotide changes. Among the five asymptomatic subjects three were mutation positive, including family II-M, VI-D, and VII-D subjects. Subject II-M was a postmenopausal female with a low level of HMBS activity in the erythrocytes and concomitant diabetes mellitus type II. Even if the diabetes has been treated, a slightly elevated serum glucose levels could exert a protective effect against overt disease (Andersson and Lithner 2001). Subjects VI-D and VII-D, females presently aged 21 and 15 years, respectively, whose HMBS activity levels in the erythrocytes were unavailable, shared identical causative mutations, which facilitated genetic counseling to prevent acute attacks. The HMBS levels in the four mutation negative subjects were within the normal range in two cases and were unavailable in the other two cases.

A total of three different novel substitutions in the PPOX gene were found in all six families with VP: c.441-442delCA in exon 5, c.917T>C [p.L306P] in exon 9, and c.1252T>C [p.C418R] in exon 12. In total, two missense mutations and one small deletion were observed in the VP families. All of the probands from families I, II, III, IV, V, and VI had positive plasma scan at 626 nm, increased levels of urinary porphyrins and their precursors PBG and

ALA. Probands from families II, III, IV, and VI had increased fecal porphyrins levels as well. A small out-of-frame deletion (c.441-442delCA) was found in family I-P1; this mutation led to a premature stop codon after the introduction of nine different amino acids. Families II-P2, III-P3, and IV-P4 shared an identical mutation (c.917T>C) that resulted in a leucine to proline substitution at position 306 (p.L306P). The V-P5 and VI-P6 probands harbored an identical change (c.1252T>C) that led to the replacement of a cysteine with proline in codon 418 (p.C418R). These three novel alterations have not been reported in reference databases (such as dbSNP, HGMD, 1KG, and ESP) and were not detected in the 96 control DNA samples. Residues L306 and C418 are located in the highly conserved FAD-binding domain (Qin et al. 2011), and these alterations most likely disrupt this interaction. The HumVar scores of 1.00 for p.L306P and 0.921 for p.C418R predicted that these mutations are most likely damaging. A small deletion (c.916_917delCT) in codon 306 has been described by Wiman et al. (2003), while no mutations have been reported in codon 418 so far. The available family members ($n = 3$ symptomatic and $n = 7$ asymptomatic) were screened for the presence of the corresponding nucleotide changes, and the details of these individuals are shown in Table 2. The symptomatic subjects III-So, IV-D, and V-Si harbored the family-specific nucleotide changes. Family III-So had an acute attack followed by chronic neurological symptoms and skin involvement and increased levels of PBG, ALA, total porphyrins in urine and feces. Family IV-D suffered from cutaneous lesions only. She had a plasma emission peak at 626 nm, normal PBG and ALA levels due to the lack of acute symptoms, and increased levels of urinary and fecal porphyrins. Family V-Si suffered from acute onset and cutaneous legions, unfortunately PBG and ALA levels shown in Table 2 were measured after the acute onset and were within normal range. However, plasma emission peak at 626 nm and increased total porphyrins in urine were observed even after the resolution of the attack. Among the seven asymptomatic subjects, four harbored the specific alterations, family I-D, II-So, IV-So, and V-Ni. Unfortunately, no biochemical data was available for the adolescent individuals I-D and V-Ni. Family II-So and IV-So had normal total porphyrins levels in urine and feces and urinary PBG and ALA levels. Plasma scan was also negative in both subjects. These results could be expected considering the fact that the significance of plasma emission peak at 626 nm is partly limited in the elderly asymptomatic carriers (IV-So). It is usually absent in asymptomatic children (II-So) (Hift et al. 2004). Unfortunately, PPOX activity could not be measured to check the cosegregation of the mutation and low enzymatic activity levels. Further analysis is needed to prove the pathogenicity of these alterations.

The majority of Bulgarian VP patients can be associated with 2 endemic regions. One of these regions is populated with ethnic Bulgarians, who are Muslim. These individuals reside in remote villages around the mountain town of Velingrad in the Rhodope mountains. Only 2 families, V and VI, from this region agreed to take part in this study, although more patients were invited. Most likely, the majority of VP patients share the identical p.C418R mutation due to consanguinity. The ancestors of families II, III, and IV originated from the small remote village of Buynovtsi, which is situated in the central Balkan mountains. Thus, a possible founder effect can also be anticipated for the p.L306P change. The endemic aggregation of families with VP and the distribution of the corresponding novel missense mutation also emphasize the pathogenic effect of these novel alterations.

A novel nonsense mutation (c.364G>T [p.E122X]) was identified in the patient with HCP shortly after her first acute attack in 2013; the details of this patient can be found in Table 2. She had increased total porphyrins levels in urine and feces and urinary PBG and ALA. Plasma scan emission peak was at 618 nm. Cutaneous involvement was absent. The p.E122X mutation is located in exon 1 and would lead to an unstable and inactive CPOX protein, which is likely removed by proteolytic degradation. The CPOX activity measurements could not be performed to prove the cosegregation of the novel alteration and low enzymatic activity.

This is the first report to describe mutations in Bulgarian patients with AIP, VP, and HCP. We identified a total of seven novel mutations in these families. Seven latent gene carriers were also detected. The identification of the latent gene carriers can result in the prevention of acute attacks by avoiding the well-known exogenic triggering factors.

Acknowledgements We would like to thank all of the families that participated in this study. We would also like to gratefully acknowledge Prof. Dimcho Adjarov for the fruitful discussions and suggestions, as well as for supplying the clinical and biochemical data used in this study. Mrs. Doroteya Leonkeva, Mrs. Kumi Kato, and Ms. Yoko Tateda are also gratefully acknowledged for their skillful technical assistance. We acknowledge the support from Ministry of Education, Culture, Sports, Science, and Technology of Japan (MEXT)

Take-Home Message

This is the first report to describe mutations in Bulgarian patients with acute hepatic porphyrias, and a total of seven novel mutations were identified in this study.

References to Electronic Databases

MIM 176000; OMIM 176200; OMIM 121300; EC 4.3.1.8; EC 1.3.3.4; EC 1.3.3.3; HMBS; PPOX; CPOX; HMBS Ensembl Accession number ENST00000442944; PPOX Ensembl Accession number ENST00000367999; CPOX Ensembl Accession number ENST00000264193; www.hgmd.cf.ac.uk

Compliance with Ethics Guidelines

Conflict of Interest

Sonya Dragneva, Monika Szyszka-Niagolov, Aneta Ivanova, Lyudmila Mateva, Rumiko Izumi, Yoko Aoki, and Yoichi Matsubara declare that they have no conflicts of interest.

Informed Consent

All procedures followed were in accordance with the ethical standards of the responsible committee on human experimentation (institutional and national) and with the Helsinki Declaration of 1975, as revised in 2000 (5). Informed consent was obtained from all patients for being included in the study.

Details of the Contribution of Individual Authors

Sonya Dragneva: involved in design, analysis, and interpretation of data, drafted the initial version of the manuscript; Monika Niagolov: involved in conception and design and critical revision of the manuscript; Aneta Ivanova: involved in conception, design, and critical revision of the manuscript; Lyudmila Mateva: involved in conception, design, and critical revision the manuscript; Rumiko Izumi: involved in analysis and interpretation of data and critical revision of the manuscript; Yoko Aoki: involved analysis and interpretation of data and critical revision of the manuscript; Yoichi Matsubara (Guarantor): involved in analysis and interpretation of data and critical revision of the manuscript

References

Adjarov DG, Naydenova EN, Kerimova MA, Pentieva ED, Ivanova LB, Ivanova VA (1994) Influence of protein calorie malnutrition and fasting on the activities of δ-aminolevulinic acid dehydratase and porphobilinogen deaminase in rats. Exp Toxicol Pathol 46:199–202

Andersson C, Lithner F (2001) Diabetic metabolism protective in severe acute intermittent porphyria. Lakartidningen 98 (51–52):5874–5876

Barbaro M, Kotajarvi M, Harper P, Floderus Y (2013) Partial protoporphyrinogen oxidase (PPOX) gene deletions, due to different Alu-mediated mechanisms, identified by MLPA analysis in patients with variegate porphyria. Orphanet J Rare Dis 8:13

Deacon AC, Elder GH (2001) Front line tests for the investigation of suspected porphyria. ACP Best Practice No 165. J Clin Pathol 54:500–507

Deybach JC, de Verneuil H, Nordmann Y (1981) The inherited enzymatic defect in porphyria variegata. Hum Genet 58 (4):425–428

Floderus Y, Shoolingin-Jordan PM, Harper P (2002) Acute intermittent porphyria in Sweden. Molecular, functional and clinical consequences of some new mutations found in the porphobilinogen deaminase gene. Clin Genet 62(4):288–297

Gill R, Kolstoe S, Mohammed F et al (2009) Structure of human porphobilinogen deaminase at 2.8 A: the molecular basis of acute intermittent porphyria. Biochem J 420(1):17–25

Hift RJ, Davidson BP, van der Hooft C, Meissner DM, Meissner PN (2004) Plasma fluorescence scanning and fecal porphyrin analysis for the diagnosis of variegate poprhyria: precise determination of sensitivity and specificity with detection of protoporphyrinogen oxidase mutations as a reference standard. Clin Chem 50(5):915–923

Hrdinka M, Puy H, Martasek P (2006) Update in porphobilinogen deaminase gene polymorphisms and mutations causing acute intermittent porphyria: comparison with the situation in Slavic population. Physiol Res 55(2):S119–S136

Kappas A, Sassa S, Galbraith RA, Nordmann Y (1995) The porphyrias. In: Scriver CR, Beaudet AL, Sly WS, Valle D (eds) Metabolic and molecular bases of inherited disease, 7th edn. McGraw-Hill, New York, vol 2, pp 2103–2159

Kauppinen R, Mustajoki S, Pihlaja H, Peltonen L, Mustajoki P (1995) Acute intermittent porphyria in Finland: 19 mutations in the porphobilinogen deaminase gene. Hum Mol Genet 4(2):215–222

Kaupinnen R, von und zu Fraunberg M (2002) Molecular and biochemical studies of acute intermittent porphyria in 196 patients and their families. Clin Chem 48(11):1891–1900

Llewellyn DH, Whatley S, Elder GH (1998) Acute intermittent porphyria caused by an arginine to histidine substitution (R26H) in the cofactor-binding cleft of porphobilinogen deaminase. Hum Mol Genet 2(8):1315–1316

Lockwood WH, Poulos V, Rossi E, Curnow DH (1985) Rapid procedure for fecal porphyrin assay. Clin Chem Jul 31 (7):1163–1167

Mauzarell D, Granick S (1956) The occurrence and determination of δ-amino-levulinic acid and porphobilinogen in urine. J Biol Chem 219(1):435–446

Meissner PN, Dailey TA, Hlft RJ, Ziman M, Corrigal AV, Roberts AG et al (1996) A R59W mutation in human protoporphyrinogen oxidase results in decreased enzyme activity and is prevalent in South Africans with variegate porphyria. Nat Genet 13(1):95–97

Meyer UA, Strand LJ, Doss M, Rees AC, Marver HS (1972) Intermittent acute porphyria – demonstration of a genetic defect in porphobilinogen metabolism. N Engl J Med 286 (24):1277–1282

Mustajoki P (1981) Normal erythrocyte uroporphyrinogen I synthase in a kindred with acute intermittent porphyria. Ann Intern Med 95(2):162–166

Paradisi I, Arias S (2010) Marked geographic aggregation of acute intermittent porphyria families carrying mutation Q180X in Venezuelan populations, with description of further mutations. J Inherit Metab Dis. doi:10.1007/s10545-010-9228-x

Puy H, Deybach JC, Lamoril J et al (1997) Molecular epidemiology and diagnosis of PBG deaminase gene defects in acute intermittent porphyria. Am J Hum Genet 60(6):1373–1383

Qin X, Tan Y, Wang L et al (2011) Structural insight into human variegate porphyria disease. FASEB J 25:653–664

Rimington C (1971) Quantitative determination of porphobilinogen and porphyrins in urine and porphyrins in faeces and erythrocytes. Assoc Clin Pathol Broadsheet 70:1–9

Sassa S (2006) Modern diagnosis and management of the porphyrias. Br J Haematol 135(3):281–292

Thunnel S, Floderus Y, Henrichson A, Harper P (2006) Porphyria in Sweden. Physiol Res 55(Suppl 2):S109–S118

To-Figueras J, Badenas C, Carrera C et al (2006) Genetic and biochemical characterization of 16 acute intermittent porphyria cases with a high prevalence of R173W mutation. J Inherit Metab Dis 29(4):580–585

Whatley SD, Puy H, Morgan R et al (1999) Variegate porphyria in Western Europe: identification of PPOX gene mutations in 104 families, extent of allelic heterogeneity, and absence of correlation between phenotype and type of mutation. Am J Hum Genet 65(4):984–994

Whatley SD, Mason NG, Woolf JR, Newcombe RG, Elder GH, Badminton MN (2009) Diagnostic strategies for autosomal dominant acute porphyrias: retrospective analysis of 467 unrelated patients referred for mutational analysis of the HMBS, CPOX, or PPOX gene. Clin Chem 55(7):1406–1414

Wiman A, Harper P, Floderus Y (2003) Nine novel mutations in the protoporphyrinogen oxidase gene in Swedish families with variegate porphyria. Clin Genet 64(2):122–130

Yang CC, Kuo HC, You HL et al (2008) HMBS mutations in Chinese patients with acute intermittent porphyria. Ann Hum Genet 72 (Pt 5):683–686

Human Molecular Genetics, 2014, Vol. 23, No. 24 **6553–6566**
doi:10.1093/hmg/ddu376
Advance Access published on July 17, 2014

New *BRAF* knockin mice provide a pathogenetic mechanism of developmental defects and a therapeutic approach in cardio-facio-cutaneous syndrome

Shin-ichi Inoue[1], Mitsuji Moriya[1], Yusuke Watanabe[4], Sachiko Miyagawa-Tomita[5,6], Tetsuya Niihori[1], Daiju Oba[1], Masao Ono[2], Shigeo Kure[3], Toshihiko Ogura[4], Yoichi Matsubara[1,7] and Yoko Aoki[1,*]

[1]Department of Medical Genetics, [2]Department of Pathology, [3]Department of Pediatrics, Tohoku University School of Medicine, Sendai, Japan, [4]Department of Developmental Neurobiology, Institute of Development, Aging and Cancer, Tohoku University, Sendai, Japan, [5]Department of Pediatric Cardiology, [6]Division of Cardiovascular Development and Differentiation, Medical Research Institute, Tokyo Women's Medical University, Tokyo, Japan and [7]National Research Institute for Child Health and Development, Tokyo, Japan

Received March 15, 2014; Revised and Accepted July 14, 2014

Cardio-facio-cutaneous (CFC) syndrome is one of the 'RASopathies', a group of phenotypically overlapping syndromes caused by germline mutations that encode components of the RAS–MAPK pathway. Germline mutations in *BRAF* cause CFC syndrome, which is characterized by heart defects, distinctive facial features and ectodermal abnormalities. To define the pathogenesis and to develop a potential therapeutic approach in CFC syndrome, we here generated new knockin mice (here $Braf^{Q241R/+}$) expressing the *Braf* Q241R mutation, which corresponds to the most frequent mutation in CFC syndrome, Q257R. $Braf^{Q241R/+}$ mice manifested embryonic/neonatal lethality, showing liver necrosis, edema and craniofacial abnormalities. Histological analysis revealed multiple heart defects, including cardiomegaly, enlarged cardiac valves, ventricular noncompaction and ventricular septal defects. $Braf^{Q241R/+}$ embryos also showed massively distended jugular lymphatic sacs and subcutaneous lymphatic vessels, demonstrating lymphatic defects in RASopathy knockin mice for the first time. Prenatal treatment with a MEK inhibitor, PD0325901, rescued the embryonic lethality with amelioration of craniofacial abnormalities and edema in $Braf^{Q241R/+}$ embryos. Unexpectedly, one surviving pup was obtained after treatment with a histone 3 demethylase inhibitor, GSK-J4, or NCDM-32b. Combination treatment with PD0325901 and GSK-J4 further increased the rescue from embryonic lethality, ameliorating enlarged cardiac valves. These results suggest that our new *Braf* knockin mice recapitulate major features of RASopathies and that epigenetic modulation as well as the inhibition of the ERK pathway will be a potential therapeutic strategy for the treatment of CFC syndrome.

INTRODUCTION

Cardio-facio-cutaneous (CFC) syndrome is an autosomal dominant congenital anomaly syndrome, characterized by a distinctive facial appearance, short stature, congenital heart defects, intellectual disability and ectodermal abnormalities such as sparse, fragile hair, hyperkeratotic skin lesions and a severe generalized ichthyosis-like condition (1). The cardiac defects observed in CFC syndrome include pulmonary valve stenosis, hypertrophic cardiomyopathy and atrial septal defects. Increased nuchal translucency/fatal cystic hygroma colli due to lymphatic defects is also occasionally observed in affected individuals (2).

*To whom correspondence should be addressed at: Department of Medical Genetics, Tohoku University School of Medicine, 1-1 Seiryo-machi, Aoba-ku, Sendai 980-8574, Japan. Tel: +81 227178139; Fax: +81 227178142; Email: aokiy@med.tohoku.ac.jp

© *The Author 2014. Published by Oxford University Press. All rights reserved.*
For Permissions, please email: journals.permissions@oup.com

Downloaded from http://hmg.oxfordjournals.org/ at National Seiiku Iryo Center on May 25, 2015

Our group as well as another group has identified germline *BRAF* mutations in 50–75% of patients with CFC syndrome (3–6). Other known CFC-causative genes include *KRAS* as well as *MAP2K1* and *MAP2K2* (MEK1 and MEK2, respectively) (3–6), all located in the same RAS–MAPK pathway that regulates cell differentiation, proliferation, survival and apoptosis (7). Germline mutations associated with RAS–MAPK pathway components cause partially overlapping disorders, including Noonan syndrome, Costello syndrome, LEOPARD syndrome, neurofibromatosis type 1 and Legius syndrome (neurofibromatosis type 1-like syndrome). These syndromes are now collectively termed RASopathies or RAS–MAPK syndromes (8–10).

BRAF is a serine threonine kinase which regulates the RAS–MAPK signaling pathway. Somatic *BRAF* mutations have been identified in 7% of human tumors, including melanoma, papillary thyroid carcinoma, colon cancer and ovarian cancer (11). The *BRAF* V600E mutation, located in the catalytic kinase domain (conserved region (CR) 3 domain), accounts for 90% of all somatic *BRAF* mutations. In contrast, *BRAF* V600E mutation has not been identified in CFC syndrome. Germline *BRAF* mutations in CR3 kinase domain, including G464R, G469E and L597V, were overlapping those in somatic mutations (4,5,12,13). In contrast, germline mutations in the CR1 domain have been rarely identified in somatic cancers. The most frequent mutations identified in CFC syndrome patients are substitutions of the residue Gln257 (p.Q257R and p.Q257K) in the CR1 domain, which account for ~40% (13). Previous studies have shown that the activation of downstream signaling, including ELK transactivation, is weaker in cells expressing the Q257R mutation than in those expressing V600E (3).

Braf is ubiquitously expressed in murine organs at mid-gestation, and high levels of its expression are found in the brain and testes at adult stage (14,15). *Braf* knockout mice have been found to die at mid-gestation from vascular defects due to enlarged blood vessels and apoptotic death of dif ferentiated endothelial cells (16). Heterozygous knockin mice constitutively expressing V600E mutation have been found to exhibit embryonic lethality (17). Knockin mice expressing a hypomorphic *BRAF* V600E allele have been reported to show phenotypes partially overlapping those of CFC syndrome patients, including small size, craniofacial abnormalities and epileptic seizures (18). However, no mouse model for CFC syndrome expressing a *Braf* mutation in the CR1 domain has been generated and no therapeutic approach has been developed. In the present study, we generated knockin mice expressing CFC syndrome-associated *Braf* Q241R mutation, corresponding to *BRAF* Q257R mutation, in order to investigate the molecular pathogenesis and potential therapeutic possibilities for CFC syndrome.

RESULTS

Generation of a CFC syndrome mouse model

We have previously reported that the transcriptional activity of ELK, downstream of ERK, was enhanced by the transient overexpression of human *BRAF* Q257R in NIH3T3 cells (3). To verify whether the expression of mouse *Braf* Q241R enhances ELK transcription as *BRAF* Q257R, reporter assays were performed in NIH3T3 cells. The expression of *Braf* Q241R and that of V637E, which corresponds to *BRAF* V600E, were ~2.7- and 8.4-fold higher than that of *Braf* WT, respectively (Fig. 1A). These results suggest that the *Braf* Q241R mutation is a gain-of-function mutation, although the activation is weaker than that observed in *Braf* V637E.

To investigate the gain-of-function effect of the *Braf* Q241R mutation on development, *Braf* Q241R knockin mice were generated (Fig. 1B). The targeting vector (Fig. 1B) was electroporated into ES cells and targeted clones were identified by Southern blotting (Fig. 1C). Appropriate ES cells were injected into BALB/c blastocysts and chimeras were obtained from six independent ES cell clones (hereafter referred to as $Braf^{Q241R\ Neo/+}$). To induce ubiquitous expression of *Braf* Q241R in germ cells, the $Braf^{Q241R\ Neo/+}$ mice were crossed with CAG-Cre transgenic mouse ($Braf^{+/+}$; *Cre*) and genotyping was confirmed by PCR (Supplementary Material, Fig. S1). Furthermore, sequencing was performed to confirm that Cre recombination resulted in *Braf* Q241R expression (Fig. 1D).

To examine if cell signaling pathways, including ERK, JNK, p38 and PI3K–AKT pathways, were altered in $Braf^{Q241R/+}$; *Cre* embryos, western blotting analysis was performed using cell extracts derived from whole-mouse embryos and brain. Protein levels of BRAF, CRAF, phosphorylated MEK and ERK in $Braf^{Q241R/+}$; *Cre* whole embryos were similar to those of $Braf^{+/+}$; *Cre* (Fig. 1E; Supplementary Material, Table S1), whereas phosphorylated MEK protein levels were higher in the brain of $Braf^{Q241R/+}$; *Cre* embryos (Fig. 1F; Supplementary Material, Table S2). Unexpectedly, phosphorylated p38 and AKT (Thr308) protein levels were somewhat lower in $Braf^{Q241R/+}$; *Cre* whole embryos at embryonic day (E) 14.5 (Fig. 1E; Supplementary Material, Table S1). These results suggest that $Braf^{Q241R/+}$; *Cre* embryos at E14.5 show a decrease of phosphorylated p38 and AKT (Thr308) protein levels.

Germline expression of *Braf* Q241R results in embryonic/neonatal lethality

Genotype analysis of embryos from an intercross between $Braf^{+/+}$; *Cre* and $Braf^{Q241R\ Neo/+}$ mice showed no surviving $Braf^{Q241R/+}$; *Cre* littermates at weaning, whereas $Braf^{+/+}$, $Braf^{+/+}$; *Cre* and $Braf^{Q241R\ Neo/+}$ littermates survived (Table 1). A normal Mendelian ratio was observed by E14.5. However, the survival rate of $Braf^{Q241R/+}$; *Cre* embryos dropped after E16.5. At E16.5, ~9.8% of embryos (4 of 41) were grossly hemorrhagic and edematous such as nuchal translucency (Fig. 2A, Table 1). Other $Braf^{Q241R/+}$; *Cre* embryos appeared normal (Fig. 2B) with no difference in body weight (data not shown). $Braf^{Q241R/+}$; *Cre* embryos, which were delivered by cesarean section at E18.5 and E19.5, remained pale and without movement or gasped for breath with cyanotic appearance, resulting in death within a few hours. A few embryos showed mandibular hypoplasia (2 of 39, 5.1%) and kyphosis (Fig. 2C and D).

Gross observation showed increased heart size in $Braf^{Q241R/+}$; *Cre* embryos at E16.5. At E18.5, $Braf^{Q241R/+}$; *Cre* embryos revealed severe peripheral liver necrosis (15 of 17, 88%) with decreased liver size and liver weight (Fig. 2E; Supplementary Material, Fig. S2). At E16.5, decreased liver weight was already observed (data not shown), although the gross appearance of the liver appeared normal. To examine if delayed lung maturation causes neonatal lethality, the histology of lung in

Downloaded from http://hmg.oxfordjournals.org/ at National Seiiku Iryo Center on May 25, 2015

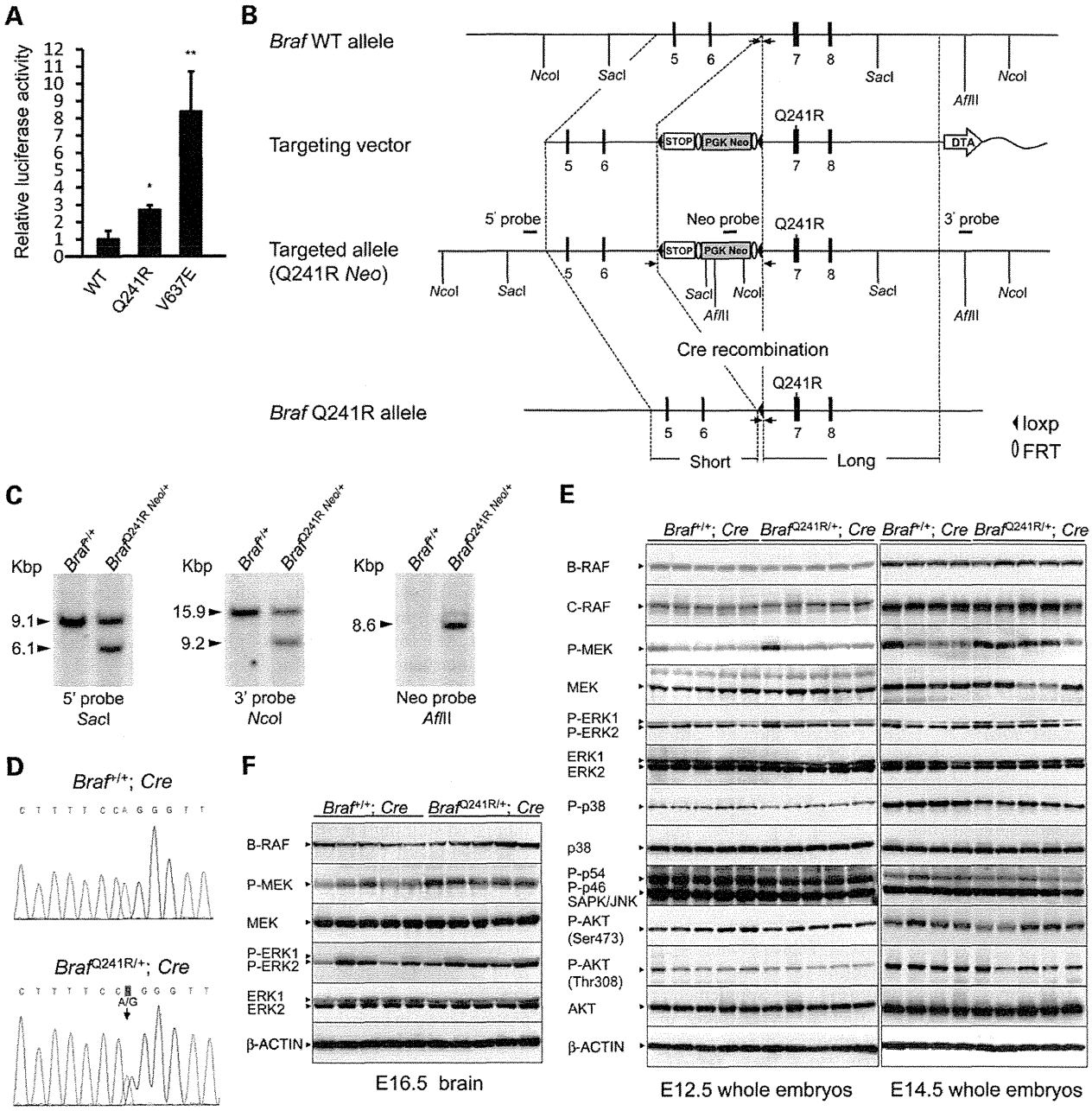

Figure 1. Generation of *Braf* Q241R knockin mice. (**A**) NIH 3T3 cells were transfected with the ELK1-GAL4 vector, the GAL4-luciferase trans-reporter vector, phRLnull-luc control vector and each mouse *Braf* expression plasmid, and reporter activities were determined as described in Materials and Methods. Luciferase activities were normalized with phRLnull-luc activities, containing distinguishable *R. reniformis* luciferase. Data are the means ± SD ($n = 4$). p.V637E in mouse *Braf* corresponds to oncogenic p.V600E in human *BRAF*. *, $P < 0.05$, **, $P < 0.01$ versus WT. WT, wild type. (**B**) Exons (solid boxes), PGK-Neomycin (PGK-Neo) cassette (gray box), STOP transcriptional sequences (open box), loxp sites (arrowheads) and Flp recombination target sites (ellipses) are indicated. Cleavage sites for diagnostic enzymes (*Sac*I, *Nco*I and *Afl*II) and the probes (5′-, 3′- and Neo probe) used to identify the homologous recombination are indicated. The PGK-Neo cassette was removed by crossing with CAG-Cre transgenic mice ($Braf^{+/+}$; *Cre*). The arrow indicates the positions of PCR primers used for genotyping of positive ES cells and mice. p. Q241R in mouse *Braf* corresponds to p.Q257R in human *BRAF*. DTA, diphtheria toxin A. (**C**) Southern blotting of ES cell clones. Genomic DNA from $Braf^{+/+}$ and $Braf^{Q241R\ Neo/+}$ ES cells was digested with *Sac*I (5′ probe), *Nco*I (3′ probe) or *Afl*II (Neo probe) and subjected to Southern blotting with a 5′, 3′ or Neo probe. The 5′, 3′ or Neo probe detects the 9.1-kb (*Braf* WT) and 6.1-kb ($Braf^{Q241R\ Neo/+}$) *Sac*I fragments, the 15.9 kb (*Braf* WT) and 9.2 kb ($Braf^{Q241R\ Neo/+}$) *Nco*I fragments or the 8.6 kb ($Braf^{Q241R\ Neo/+}$) *Afl*II fragment, respectively. (**D**) RNA was isolated from the brain of $Braf^{+/+}$; *Cre* and $Braf^{Q241R/+}$; *Cre* embryos at E18.5, and reverse transcribed into cDNA. Sanger sequencing was carried out using the cDNA. The arrow indicates the Q241R mutation in *Braf* exon 7. (**E** and **F**) Protein extracts from whole-mouse embryos (E12.5 and E14.5) and brain (E16.5) ($n = 4–5$ of each genotype) were subjected to western blotting with the indicated antibodies. β-Actin is shown as a loading control. The arrowheads indicate the bands corresponding to each protein.

Downloaded from http://hmg.oxfordjournals.org/ at National Seiiku Iryo Center on May 25, 2015

Table 1. Genotyping of pups resulting from intercross between *Braf*$^{+/+}$; *Cre* and *Braf*$^{Q241R\ Neo/+}$ mice

Age	*Braf*$^{+/+}$	*Braf*$^{+/+}$; *Cre*	*Braf*$^{Q241R\ Neo/+}$	*Braf*$^{Q241R/+}$; *Cre*	*n*	*P*
E12.5	24	29	23	23	99	0.80
E13.5	5	14	6	6 (2 [1])	31	0.08
E14.5	19	22 (1)	23	11 (1 [1])	75	0.19
E16.5	57	60	55	34 (7 [4])	206	0.04
E18.5	16	23	20	0 (17 [4])	59	<0.0001
E19.5	11	16	11	0 (11 [1])	38	<0.01
Weaning (P21)	56	54	56	0	166	<0.0001
Expected	25%	25%	25%	25%		

Deviation from the expected Mendelian ratios was assessed by the χ^2 test. The number of dead embryos is shown in parentheses. The number of edematous embryos is shown in brackets. P: postnatal day.

Braf$^{Q241R/+}$; *Cre* embryos was examined at E18.5 and E19.5. Lungs of the mutant embryos appeared normal and were able to inflate, but ~11.1% of embryos (1 of 9) showed alveolar hemorrhage (Supplementary Material, Fig. S3). Thyroid transcription factor-1 (TTF-1; lung epithelial cells marker), pro-surfactant protein C and PAS staining showed similar levels in *Braf*$^{Q241R\ Neo/+}$ and *Braf*$^{Q241R/+}$; *Cre* embryos (Supplementary Material, Fig. S4), suggesting that lung development and maturation are normal. Gross observation suggests that *Braf*$^{Q241R/+}$; *Cre* embryos show embryonic/neonatal lethality, cardiomegaly, liver necrosis, edema and craniofacial abnormalities.

Braf$^{Q241R/+}$; *Cre* embryos display various heart defects

Because *Braf*$^{Q241R/+}$; *Cre* embryos showed cardiomegaly and liver necrosis, possibly due to heart failure (Fig. 2E), detailed histological analysis of the heart at different embryonic stages was conducted. At E12.5, the hearts of *Braf*$^{Q241R/+}$; *Cre* embryos appeared normal (Supplementary Material, Fig. S5A), but showed an enlarged pulmonary valve and a dramatic increase in the density of trabeculae (hypertrabeculation) at E14.5 (Supplementary Material, Fig. S5B). At E16.5, 13 of 14 (93%) *Braf*$^{Q241R/+}$; *Cre* embryos (excluding edematous embryos) had various heart defects (Supplementary Material, Tables S3 and S4). Hypertrophy of pulmonary, tricuspid and mitral valves was present in 7, 8 and 9 of 14 embryos, respectively (Fig. 3A; Supplementary Material, Tables S3 and S4). In particular, hypertrophy in pulmonary valve leaflets was prominent, plugging the entire space of the pulmonary valve ring (Fig. 3B). Other heart defects observed in *Braf*$^{Q241R/+}$; *Cre* embryos included ventricular septal defect (VSD) in 2 of 14 embryos (Fig. 3A), abnormal endocardial cushion in 2 (Fig. 3A), hypertrabeculation in 3 (Fig. 3A), epicardial blisters in 2 (Fig. 3A and C), a thickened trabecular layer and thinned compact layer in the left, right or combined myocardium (noncompaction: one case of cardiomyopathy accompanied by cardiac hypertrophy) in 4 (Fig. 3D) and hypoplasia of the coronary arteries in 3. The ventricular radius and the thickness of the pulmonary and tricuspid valves were significantly higher in *Braf*$^{Q241R/+}$; *Cre* embryos, suggesting cardiac enlargement and thickened pulmonary and tricuspid valves (Fig. 3E). These results suggest that *Braf*$^{Q241R/+}$; *Cre* embryos develop various congenital heart defects, which almost certainly contributes to embryonic lethality.

Braf$^{Q241R/+}$; *Cre* embryo hearts exhibit enhancement of cell proliferation, ERK signaling activation and decrease of phosphorylated p38 and AKT

To examine if heart defects observed in *Braf*$^{Q241R/+}$; *Cre* embryos are caused by increased cell proliferation and/or reduced cell death, cell proliferation was analyzed by phosphohistone H3 (pHH3) immunostaining and cell death by TUNEL assay. At E13.5, regarding heart abnormalities in each embryos, the number of pHH3-positive-stained cells varied. pHH3-positive-stained cells in the interventricular septum and myocardium increased in *Braf*$^{Q241R/+}$; *Cre* embryos (Fig. 4A and B). At E16.5, the nucleus of pHH3-positive cells increased in the interventricular septum in embryos with VSD (Fig. 4C). *Braf*$^{Q241R/+}$; *Cre* embryos had more pHH3-positive cells in pulmonary valves (Fig. 4D). In contrast to cell proliferation, hardly any cells undergoing apoptosis were observed in either *Braf*$^{+/+}$; *Cre* or *Braf*$^{Q241R/+}$; *Cre* at E13.5 and E16.5 (data not shown). These results suggest that the cell proliferation state depends on heart abnormalities in each embryo at E16.5 and that the increased staining for pHH3 in the interventricular septum was associated with VSD.

To examine if the cardiac signaling pathways were altered in *Braf*$^{Q241R/+}$; *Cre* embryos, the activation of kinases was screened in various signaling pathways using a phospho-kinase array followed by western blotting of the lysates from hearts of *Braf*$^{Q241R/+}$; *Cre* embryos at E16.5 (Fig. 4E and F; Supplementary Material, Fig. S6). No changes in phosphorylated ERK protein levels in both the phospho-kinase array and western blotting were observed. In contrast, phosphorylated p38, AKT (Ser473) and AKT (Thr308) protein levels, which are not direct targets of BRAF, were relatively lower in *Braf*$^{Q241R/+}$; *Cre* embryos than in *Braf*$^{+/+}$; *Cre*, which was confirmed by western blotting. To verify the activation of transcription factors downstream of ERK, the expression of ELK1 and the PEA3 (polyoma enhancer activator 3) subfamily Ets transcription factors were examined by quantitative real-time PCR, these expressions being known as transcriptional targets of FGF signaling-mediated activation of ERK in heart and oncogenic BRAF signaling in melanoma (19,20). At E13.5, E16.5 and E18.5, cardiac mRNA levels of *Etv1*, *Etv4* and *Etv5*, but not *Elk1*, were significantly higher in *Braf*$^{Q241R/+}$; *Cre* embryos than those in *Braf*$^{+/+}$; *Cre* (Fig. 4G; Supplementary Material, Fig. S7). Next, we investigated the influence of genes responsible for hypertrophic cardiomyopathy and

Downloaded from http://hmg.oxfordjournals.org/ at National Seiiku Iryo Center on May 25, 2015